Distribution of Water and Counterions in Vermiculite Clays

Kenneth S. Schmitz

Department of Chemistry, University of Missouri−Kansas City, Kansas City, Missouri 64110

Received: August 16, 1999; In Final Form: August 24, 1999

Williams, Soper, Skipper, and Smalley (*J. Phys. Chem. B* **1998**, *102*, 8945) reported neutron scattering results on the counterion−water distribution vermiculite clay surfaces, in which a bilayer of water was found to be preferred at the surface rather than the counterions. This observation is in contrast to the predictions of the Poisson−Boltzmann equation, as pointed out by these authors. We report calculations on a one-dimensional adsorption model that includes nearest-neighbor interactions for the competition between water and the counterion for the lattice site of the clay surface. The association for either species is assumed to be of electrostatic origin, where the molecular parameters are based on the known structures of water, the counterion, and the clay surface. With no adjustable parameters these calculations indicate that less than 15% of the sites are "bound" with the counterions. These results suggest that it is the much larger concentration of the water and the confined volume between the clay surfaces that is responsible for the reported water−counterion distribution.

1. Introduction

Recently Williams et al.[1] reported a high-resolution study on the distribution of water and counterions in the double-layer region of vermiculite clays. The clay used in this study was from Eucatex, Brazil, with the reported composition

$$[Si_{3.07}Mg_{2.72}Al_{0.83}Fe_{0.25}Ti_{0.06}Ca_{0.06}Cr_{0.005}K_{0.005}O_{10}\text{-}(OH)_2]M_{0.65}{}^{+}\cdot nH_2O \quad (1)$$

where M^+ is the neutralizing cation. The above formula corresponds to only one of the two exposed surfaces of the structural unit of the clay, which has dimensions of 9 Å × 5 Å. Therefore the surface charge density is $\sigma = 0.65 \times 1.6 \times 10^{-19}/9 \times 5 \times 10^{-20} = 0.23$ C m^{-2} on each exposed face.

The swelling of clays is due to the hydration of the cation, which forces the clay layers apart. However the propylammonium cation ($C_3H_7NH_3^+$) induces very large volumes of water to be drawn between the clay plates. In the studies by Williams and co-workers the clays were first soaked in 1 M NaCl to remove the naturally occurring counterions and then treated with $C_3H_7NH_3Cl$ to obtain propylammonium Eucatex. The clays were then swollen in D_2O, and counterions were displaced with either $C_3H_7ND_3^+$ or $C_3D_7ND_3^+$ as the cation M^+ in eq 1.

Neutron scattering data indicated a surface-to-surface distance of approximately 43.6 Å. The scattering data for density profiles normal to the clay layers clearly show two layers of water at the clay layer surfaces and a broad distribution of the counterions between the layers with *a maximum in the midplane region*. This distribution of the counterions was stated to be contrary to the predictions of the Poisson−Boltzmann (PB) equation.

To estimate the predictions of the PB equation we use the theory of Engström and Wennerström,[2] who obtained an analytical solution for parallel charged plates. They distinguished between the ions "trapped" near the surface due to the interaction energy being greater than the thermal energy k_BT, where k_B is Boltzmann's constant and T is the absolute temperature, and those counterions physically located on the surface. For the latter quantity they obtained for the density of surface-bound counterions ρ_s

$$\rho_s = \frac{2\epsilon_r\epsilon_0 k_B T s^2}{Z_c q_e a^2} \frac{(\sigma Z_c q_e a)^2}{(2\epsilon_r\epsilon_0 k_B T s)^2 + 1} \quad (2)$$

where in our notation ϵ_r is the relative permittivity, ϵ_0 is the permittivity of the vacuum, q_e is the magnitude of the electron charge, σ is the surface charge density, Z_c is the counterion charge number, $2a$ is the distance between the two plates, and s is a dimensionless parameter given by

$$s = a\sqrt{\frac{n_c Z_c q_e}{2k_B T\epsilon_r\epsilon_0}} \quad (3)$$

where n_c is the number concentration of counterions. The fraction of "contact" counterions, f_c, was obtained by integration of the charge density over the region from the surface to a distance Δ, the latter being the dimension of the counterions. They obtained the expression

$$f_c = 1 - \frac{1}{1 - \dfrac{\Delta\sigma Z_c q_e}{2\epsilon_r\epsilon_0 k_B T}} \quad (4)$$

Of particular interest in the present study is the value of f_c for plate separation distances of $2a < 50$ Å. We use $\sigma = 0.2$ C m^{-2} as an estimate for the vermiculite surface charge density and a thickness $\Delta = 3$ Å to represent the diameter of the counterion. From eq 4 the fraction of surface sites bound with counterions is expected to be in excess of 0.63. This theoretical prediction clearly does not agree with neutron scattering results of Williams and co-workers.[1]

Williams et al. explanation of the counterion distribution was that the "hydrated surfaces" of two water molecules thick were responsible for the counterion distribution to be maximized between the clay surfaces. This view, however, is an *ex post*

10.1021/jp992894j CCC: $18.00
Published on Web 10/01/1999

facto interpretation with the implication that the "hydration forces" are stronger than the electrostatic forces between the surface and the counterions.

We examine herein the competitive adsorption between water and counterions for sites on a charged surface. The matrix method is used to generate exactly all possible configurations that contribute to the grand partition function, in which nearest-neighbor interactions are included.[3] The interaction energies are assumed to be solely of unscreened electrical origin and based on reasonable water and counterion dimensions.

2. Adsorbing Species

Williams et al. presented two neutron scattering profiles, one with isotopic substitution and one without. They described the distribution of water and counterions by both the intensity and the positions of the scattering peaks. They stated that peaks in the range 0−3.3 Å are due to atoms in the crystalline clay structure because of the deuterium exchange. The strong common peaks that occur at 6.6 and 9.6 Å are attributed to water, as is also a weaker peak at 12.6 Å. These positions are consistent with a water radius of 1.5 Å. A weaker peak appeared at 11.2 Å, about which they stated that a small proportion of the ND_3^+ headgroups of the counterions were also incorporated into the second layer of water.

From the above account of the data one may conclude that there was an absence of counterions in direct contact with the surface with only a slight presence in the second water layer. One interpretation of these observations is that the adsorption of water onto the surface is so great that the counterions are totally excluded. A second interpretation is that the counterions themselves are hydrated and it is the hydrated unit that is in competition with the solvent for sites on the clay surface. We next examine the electrostatic interactions on this structural information.

3. Coulomb Interactions Based on Structural Information

The unit clay cell has dimensions of 9 Å × 5 Å × 10 Å and a net charge of $Z = 1.3$. Hence there are 0.65 charge units on one face of dimensions 9 Å × 5 Å. If the charges are assumed to be uniformly distributed, then the average linear charge separation is $b = 8.3$ Å. From the neutron scattering data the region assigned to the atoms in the clay is 3.3 Å thick. We therefore locate this site charge $Z_s = -1$ a distance of $r_s = 1.52$ Å below the surface to reflect the finite size of the charge group.

We next consider the counterion species $C_3H_7ND_3^+$ or $C_3D_7ND_3^+$. Since the charged groups lie at one end of these molecules, we assume they are oriented as to have these groups nearest the surface. From the neutron scattering data with the first water peak at 6.6 Å and the second peak associated with the cation at 11.2 Å we may assign the value of $r_c = 1.60$ Å as the location of the counterion charge $Z_c = +1$ from the headgroup surface. The partial molar volume of *n*-butylammonium is about 150 Å^3 (M. Smalley, personal communication). If we represent the cation as an equivalent cylinder and take the headgroup dimension as representative of the radius, then the length of the cation is ≈18.7 Å with $r_c = 1.60$ Å (cylindrical model). However, the cation may be represented as an equivalent sphere with an effective radius of ≈5.3 Å, in which case $r_c = 5.33$ Å (spherical model).

Water is electrically neutral but exhibits a dipolar charge distribution. The partial charge for water is estimated from the dipole moment of 1.87×10^{-18} esu[3]. If we assume a radius for a water molecule of $r_w = 1.50$ Å and a charge separation distance $r_{sep} = 1.50$ Å, then we obtain two partial charges of magnitude $|\delta Z_w| = 0.26$ that are separated by a distance $r_d = 0.75$ Å.

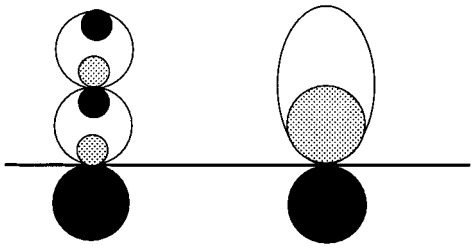

Figure 1. Nearest-neighbor model for water−counterion adsorption The surface ion groups are represented by the filled circles, with centers located a distance r_s from the surface and have a lattice spacing of b. The counterions are elongated to represent the carbon chain, and the ammonium group is indicated by the dotted circle of radius r_c. The single water molecule of radius r_w is represented by two internal circles whose interior reflects the sign of the partial charge distribution. Shown above is a bilayer of water as indicated from neutron scattering profiles.

A schematic representation of the clay surface, two layers of water, and the counterion is given in Figure 1.

4. Boltzmann Weighting Factors

The greatest distance from the surface charge that we are considering is the hydrated counterion, where the distance is $r_s + 2r_w + r_c = 6.1$ Å (cylindrical model of the counterion). The lattice sites along the linear surface are estimated to be 8.3 Å apart. Since the distance examined perpendicular to the site is comparable to the separation distance between nearest neighbors along the lattice, nearest-neighbor interactions may play a factor in the determination of the extent of site coverage. We now construct the energies of interaction for ligands and the surface and also nearest-neighbor pairs.

The equilibrium between the species on the lattice and in solution is determined by equating the chemical potentials of both phases. It is assumed that in the solution phase Henry's law prevails and the components are assumed to be ideal. Since there are two layers of water and the counterion is found in the second layer, the state at each "lattice site" is represented as a two-layer system. Thus the state of each lattice site is composed of two substates corresponding to the first and second layer. The state of the lattice site is denoted by (X,Y), where X is the state of the first layer and Y is the state of the second layer. For our system there are three possibilities: an empty location, denoted by "0"; bound water, denoted by "1"; and the headgroup of the bound counterion, denoted by "2".

Our ultimate goal is to construct a matrix for generating the exact configuration of all allowed states in a linear lattice and thereby to calculate the grand partition function and the fraction of sites bound by each of the allowed states. We define as our reference state the unbound lattice. If the first layer is unbound, then the second layer is also taken to be unbound. The reference state is symbolized as (0,0) and given the site index "1". The second state of interest is the hydration state of the lattice in which two layers of water are present, which is denoted by (1,1). This hydrated state is given the site index "2". The third state is the bound ligand in which a water molecule is in layer 1 and the headgroup in layer 2 and denoted by (1,2). Note that this also represents the adsorption of hydrated counterions with an orientation dictated by the experimental data. This site state (1,2) is denoted by "3". The fourth and fifth site state are not reported in the data but included in the present calculations for completeness. This fourth site state is that in which the headgroup is in layer 1. Due to the fact that the bilayer is about 6 Å thick and

the extension of the counterion could be as great as 18.7 Å as estimated in the previous paragraph, there is no water in the second layer. This fourth state is thus represent by (2,0) and denoted by the site index "4". The fifth site state is simply a water molecule in layer 1 but nothing in layer 2 (empty location). This site state is represented as (1,0) and given the site index "5".

Surface−Ligand Interactions. We assign the symbols K_α and L_α to indicate the interaction of water or counterion, respectively, in the α layer with the clay surface. For dipolar water in the first layer above the *j*th site with interaction in the $j + 1$ and $j - 1$ surface sites we define the parameter K_1 by the total Coulomb energy,

$$\ln(K_1) = -\lambda_B|\delta Z_w Z_s|\left(\frac{1}{r_s + 2r_w - r_d} - \frac{1}{r_s + r_d} + \frac{2}{\sqrt{(r_s + 2r_w - r_d)^2 + b^2}} - \frac{2}{\sqrt{(r_s + r_d)^2 + b^2}}\right) \quad (5)$$

where $\lambda_B = q_e^2/4\pi\epsilon_r\epsilon_0 k_B T$ is the Bjerrum length and || indicates the absolute value. The association parameter for water in the second layer is given by

$$\ln(K_2) = -\lambda_B|\delta Z_w Z_s|\left(\frac{1}{r_s + 4r_w - r_d} - \frac{1}{r_s + r_d + 2r_w} + \frac{2}{\sqrt{(r_s + 4r_w - r_d)^2 + b^2}} - \frac{2}{\sqrt{(r_s + 2r_w + r_d)^2 + b^2}}\right) \quad (6)$$

Since water is assumed to be a monomer in solution, there is an additional interaction term between the two water molecules in the bilayer that constitutes site state 2 for the lattice, viz.,

$$\ln(K_{12}) = -\lambda_B(\delta Z_w)^2\left(\frac{2}{2r_w} - \frac{1}{2r_d} - \frac{1}{4r_w - 2r_d}\right) \quad (7)$$

The corresponding weighting factors for the counterion interactions with the surface are, for site state 4 in which the counterion is restricted to the first layer,

$$\ln(L_1) = -\lambda_B|Z_c Z_s|\left(-\frac{1}{r_s + r_c} - \frac{2}{\sqrt{(r_s + r_c)^2 + b^2}}\right) \quad (8)$$

and, for the counterion in the second layer,

$$\ln(L_2) = -\lambda_B|Z_c Z_s|\left(-\frac{1}{r_s + 2r_w + r_c} - \frac{2}{\sqrt{(r_s + 2r_w + r_c)^2 + b^2}}\right) \quad (9)$$

If the counterion is hydrated in solution, then there is no additional interaction energy between the water in layer 1 and the headgroup in layer 2. However, if the counterion is not hydrated in solution, then there is an additional interaction between the two species in site state 3, denoted by L_h and given by

$$\ln(L_h) = -\lambda_B|\delta Z_w Z_c|\left(\frac{1}{2r_w - r_d + r_c} - \frac{1}{r_c + r_d}\right) \quad (10)$$

There is one other factor that establishes the equilibrium between the lattice and solution phases, and that is the concentration of the free species. The concentration factors m_j/55.5 arise from Henry's Law with the pure solvent as the reference state. Hence we have the following Boltzmann weighting factors for the four allowed states:

$$B_1 = 1 \quad \text{[surface state (0,0)]} \quad (11)$$

$$B_2 = \left(\frac{m_w}{55.5}\right)^2 K_1 K_2 K_{12} \quad \text{[surface state (1,1)]} \quad (12)$$

$$B_3 = \begin{cases} \left(\frac{m_w}{55.5}\right)\left(\frac{m_c}{55.5}\right)K_1 L_2 L_h & \text{(unhydrated)} \\ \left(\frac{m_c}{55.5}\right)K_1 L_2 & \text{(hydrated)} \end{cases} \quad \text{[surface state (1,2)]} \quad (13)$$

$$B_4 = \left(\frac{m_c}{55.5}\right)L_1 \quad \text{[surface state (2,0)]} \quad (14)$$

and

$$B_5 = \left(\frac{m_w}{55.5}\right)K_1 \quad \text{[surface state (1,0)]} \quad (15)$$

Nearest-Neighbor Interaction. The next factors to consider are the nearest-neighbor interaction terms. Whenever a vacant site is one of the pair of sites, then the nearest-neighbor interaction is defined as zero as this is the standard state. Hence $W_{11} = W_{1j} = W_{j1} = 1$ is the weighting factor. Using the above scheme for site indices, we have for following nearest-neighbor interactions:

$$\ln(W_{22}) = -\lambda_B(\delta Z_w)^2\left(\frac{4}{b} + \frac{4}{\sqrt{(2r_w)^2 + b^2}} - \frac{4}{\sqrt{(2r_w - 2r_d)^2 + b^2}} - \frac{2}{\sqrt{(4r_w - 2r_d)^2 + b^2}} - \frac{2}{\sqrt{(2r_d)^2 + b^2}}\right) \quad (16)$$

$$\ln(W_{23}) = \ln(W_{32}) = -\lambda_B\left[(\delta Z_w)^2\left(\frac{2}{b} + \frac{2}{\sqrt{(2r_w)^2 + b^2}} - \frac{2}{\sqrt{(2r_w - 2r_d)^2 + b^2}} - \frac{1}{\sqrt{(2r_d)^2 + b^2}} - \frac{1}{\sqrt{(4r_w - 2r_d)^2 + b^2}}\right) + |\delta Z_w Z_c|\left(\frac{1}{\sqrt{(2r_w + r_c - r_d)^2 + b^2}} + \frac{1}{\sqrt{(r_c - r_d)^2 + b^2}} - \frac{1}{\sqrt{(2r_w - r_c - r_d)^2 + b^2}} - \frac{1}{\sqrt{(r_c + r_d)^2 + b^2}}\right)\right] \quad (17)$$

$$\ln(W_{24}) = \ln(W_{42}) = -\lambda_B\left[|\delta Z_w Z_c|\left(\frac{1}{\sqrt{(2r_w + r_d - r_c)^2 + b^2}} + \frac{1}{\sqrt{(r_c - r_d)^2 + b^2}} - \frac{1}{\sqrt{(2r_w - r_d - r_c)^2 + b^2}} - \frac{1}{\sqrt{(4r_w - r_d - r_c)^2 + b^2}}\right)\right] \quad (18)$$

$$\ln(W_{25}) = \ln(W_{52}) = -\lambda_B(\delta Z_w)^2\left(\frac{2}{b} + \frac{2}{\sqrt{(2r_w)^2 + b^2}} - \frac{2}{\sqrt{(2r_w - 2r_d)^2 + b^2}} - \frac{1}{\sqrt{(4r_w - 2r_d)^2 + b^2}} - \frac{1}{\sqrt{(2r_d)^2 + b^2}}\right) \quad (19)$$

$$\ln(W_{33}) = -\lambda_B\left[|\delta Z_w Z_c|\left(\frac{2}{\sqrt{(2r_w + r_c - r_d)^2 + b^2}} - \frac{2}{\sqrt{(r_c + r_d)^2 + b^2}}\right) + (\delta Z_w)^2\left(\frac{2}{b} - \frac{2}{\sqrt{(2r_w - 2r_d)^2 + b^2}}\right) + \frac{Z_c^2}{b}\right] \quad (20)$$

$$\ln(W_{34}) = \ln(W_{43}) = -\lambda_B\left[|\delta Z_w Z_c|\left(\frac{1}{\sqrt{(r_c - r_d)^2 + b^2}} - \frac{1}{\sqrt{(2r_w - r_c - r_d)^2 + b^2}}\right) + \frac{Z_c^2}{\sqrt{(2r_w)^2 + b^2}}\right] \quad (21)$$

$$\ln(W_{35}) = \ln(W_{53}) = -\lambda_B\left[(\delta Z_w)^2\left(\frac{2}{b} - \frac{2}{\sqrt{(2r_w - 2r_d)^2 + b^2}}\right) + |\delta Z_w Z_c|\left(\frac{1}{\sqrt{(2r_w + r_c - r_d)^2 + b^2}} - \frac{1}{\sqrt{(r_c + r_d)^2 + b^2}}\right)\right] \quad (22)$$

$$\ln(W_{44}) = -\frac{\lambda_B Z_c^2}{b} \quad (23)$$

$$\ln(W_{45}) = \ln(W_{54}) = -\lambda_B|\delta Z_w Z_c|\left(\frac{1}{\sqrt{(r_c - r_d)^2 + b^2}} - \frac{1}{\sqrt{(2r_w - r_c - r_d)^2 + b^2}}\right) \quad (24)$$

$$\ln(W_{55}) = -\lambda_B(\delta Z_w)^2\left(\frac{2}{b} - \frac{2}{\sqrt{(2r_w - 2r_d)^2 + b^2}}\right) \quad (25)$$

We now have all of the necessary weighting factors for our model. The next step is to generate the grand partition function using these factors.

5. Matrix Generation of the Grand Partition Function

The adsorption isotherm for a system of N identical sites is calculated from the grand partition function Ξ using the general formula[4]

$$\theta_j = \frac{1}{N}\frac{\partial \ln(\Xi)}{\partial \ln(m_j)} \quad (26)$$

where θ_j is the fraction of sites occupied by the jth species of molality m_j. We assumed a one-dimensional lattice model with nearest-neighbor interactions since the grand partition can be calculated exactly.

The generating matrix is obtained as follows.[5] We construct a table consisting of a column and row consisting of the five states 1, 2, 3, and 4 and 5. The column represents the state at site j and the row represents the state at site $j + 1$. The elements of the table, hence the generation matrix, represent the Boltzmann weighting factor for the addition of site $j+1$ to a preexisting chain with the state at site j. Following these rules we obtain the expression for generating Ξ,

$$\Xi = (1,0,0,0,0)\cdot\mathbf{M}^N\cdot\begin{pmatrix}1\\1\\1\\1\\1\end{pmatrix} = (1,0,0,0,0)\cdot\begin{bmatrix}1 & B_2 & B_3 & B_4 & B_5\\ 1 & B_2W_{22} & B_3W_{23} & B_4W_{24} & B_5W_{25}\\ 1 & B_2W_{32} & B_3W_{33} & B_4W_{34} & B_5W_{35}\\ 1 & B_2W_{42} & B_3W_{43} & B_4W_{44} & B_5W_{45}\\ 1 & B_2W_{52} & B_3W_{53} & B_4W_{54} & B_5W_{55}\end{bmatrix}^N\cdot\begin{pmatrix}1\\1\\1\\1\\1\end{pmatrix} \quad (27)$$

Rather than work with the matrix multiplication, we can use the largest eigenvalue to calculate θ_j,

$$\theta_j = \frac{\log[\lambda_+(m_j + \delta m_j)] - \log[\lambda_+(m_j - \delta m_j)]}{\log[m_j + \delta m_j] - \log[m_j - \delta m_j]} \quad (28)$$

where λ_+(m) is the largest eigenvalue of the generating matrix and the derivative is estimated on the computer by the finite difference method. This expression gives the fraction of sites occupied by the total number of states for any one species. We wish to distinguish between "hydrated" and "unhydrated" counterions. We can calculate the fraction of sites in a particular site state α by taking the derivative with respect to B_α. Hence the desired adsorption fractions are calculated by

$$\theta_j = \frac{\log[\lambda_+(B_j + \delta B_j)] - \log[\lambda_+(B_j - \delta B_j)]}{\log[B_j + \delta B_j] - \log[B_j - \delta B_j]} = \frac{B_j}{\lambda_+(B_j)}\frac{\lambda_+(B_j + \delta B_j) - \lambda_+(B_j - \delta B_j)}{2\delta B_j} \quad (29)$$

6. Numerical Evaluation of θ_j

All of the energy parameters are fixed by the geometries described in section 3 and the equations in section 4. Since the concentration is based on the molality, we have $m_w = 55.5$. The concentration of the counterion is estimated from the surface charge density and the distance between the clay surfaces. In the present case the surfaces of the clay plates are separated by a distance of $2a \approx 34$ Å after correcting for the thickness of the clay. The surface area of 8.3 Å × 8.3 Å per counterion yields a volume of 2342 Å^3 for both counterions. This gives a molar concentration of 1.42 M, which we take as the molal concentration $m_c \approx 1.42$ m in our calculations.

The counterion is represented in these calculations by the cylindrical model for which $r_c = 1.60$ Å. This choice, rather than the spherical counterion value of $r_c = 5.33$ Å, is to maximize the extent of adsorption of the counterion. Hence if the cylindrical model fails to achieve the coverage predicted by the PB equation, then the spherical model would be even further from the PB prediction.

Calculations were performed with all five site states mentioned above. Model 1 assumes that the counterion is hydrated in solution whereas model 2 includes the water−counterion interaction at the site as the counterions are assumed to be unhydrated in solution. Both models 1 and 2 include site states not reported in the Williams et al. study, viz, in which the headgroup is in the first layer (site state 4) and there is water in the first layer with a vacant second layer (site state 5). We also did calculations in which only states 1, 2, and 3 are allowed by eliminating the fourth and fifth rows and columns in the

TABLE 1: Site−Ligand Interaction Parameters for Each Layer in the Cylindrical Counterion Model[a]

K_1	K_2	K_{12}	L_1	L_2	L_h
1.4173	1.1149	1.1129	21.8938	6.3888	1.3594

[a] Calculated with the following parameters: $r_c = 1.60$ Å; $r_s = 1.52$ Å; $r_d = 0.75$ Å; $r_w = 1.50$ Å; $Z_s = -1$, $Z_c = +1$; $|\delta Z_w| = 0.26$.

TABLE 2: Site−Ligand Combination Interaction Parameters for the Cylindrical Counterion Model[a]

$\frac{B_2}{(m_w/55.5)^2}$	=	$K_1K_2K_{12}$	=	1.7586
$\frac{B_3}{(m_c/55.5)(m_w/55.5)}$	=	$K_1L_2L_h$	=	12.3087
$\frac{B_3}{(m_c/55.5)}$	=	K_1L_2	=	9.0546[b]
$\frac{B_4}{(m_c/55.5)}$	=	L_1	=	21.8938
$\frac{B_5}{(m_w/55.5)}$	=	K_1	=	1.4173

[a] Calculated with the following parameters: $r_c = 1.60$ Å; $r_s = 1.52$ Å; $r_d = 0.75$ Å; $r_w = 1.50$ Å; $Z_s = -1$, $Z_c = +1$; $|\delta Z_w| = 0.26$. [b] Hydration model in which the water and counterion are associated in the solution.

TABLE 3: Nearest-Neighbor Interaction Parameters W_{ij} for the Cylindrical Counterion Model ($W_{ij} = W_{ji}$)[a]

	j			
i	2	3	4	5
2	0.9943	1.0099	0.9888	0.9971
3		0.4327	0.4464	1.0057
4			0.4239	1.0005
5				0.9981

[a] Calculated with the following parameters: $r_c = 1.60$ Å; $r_s = 1.52$ Å; $r_d = 0.75$ Å; $r_w = 1.50$ Å; $b = 10.3$ Å; $Z_s = -1$, $Z_c = +1$; $|\delta Z_w| = 0.26$.

generation matrix. Models 3 and 4 are, respectively, the three site state system with and without hydrated counterions.

All calculations were done using *Mathematica*, a means of doing mathematics on the computer. After construction of the generating matrix and substitution of the numerical values of the parameters, the largest root was obtained from the package *Eigenvalues*.

Shown in Table 1 are the surface−ligand interaction parameters for the two different layers, and in Table 2 are the concentration-independent parts of the B_j parameters. Summarized in Table 3 are the nearest-neighbor interaction parameters W_{ij}, where $i, j \geq 2$, since $W_{i1} = W_{1j} = W_{11} = 1$. The fraction of sites for each species is given in Table 4 for four different models.

7. Discussion

On the basis of the Poisson−Boltzmann equation, Engström and Wennerström[2] obtained an expression to estimate the fraction of a surface occupied by counterions for a given surface charge density. Using reasonable parameters for vermiculite clay, the anticipated coverage calculated from eq 4 is $f_c \approx 0.6$ for a thickness of 3 Å. The experimental data of Williams et al.[1] quite clearly indicated that this fraction is not even

TABLE 4: Fraction of State-Specific Sites Occupied for the Cylindrical Counterion Model[a]

model no.	θ_1	θ_2	θ_3	θ_4	θ_5	$\theta_2+\theta_5$	$\theta_3+\theta_4$
1[b]	0.2052	0.3647	0.0410	0.0964	0.2928	0.6575	0.1374
2	0.2045	0.3601	0.0546	0.0937	0.2891	0.6492	0.1483
3[b]	0.3335	0.5941	0.0724			0.5941	0.0724
4	0.3256	0.5803	0.0942			0.5803	0.0942

[a] Calculated with the following parameters: $r_c = 1.60$ Å; $r_s = 1.52$ Å; $r_d = 0.75$ Å; $r_w = 1.50$ Å; $Z_s = -1$, $Z_c = +1$; $|\delta Z_w| = 0.26$. [b] Hydrated counterion.

approached even up to a thickness of 6 Å. Furthermore, their neutron scattering profiles showed that the maximum in the distribution of counterions occurred midway between the two clay plates. They attributed this observation to "hydration forces" as an *ex post facto* observation that two layers of water molecules intervened between the clay surface and the headgroup of the counterions, with an occasional peeping through of a headgroup into the second layer.

We refer to the work of Henderson and co-workers[6−9] on hydration forces that are attributed to the hard sphere nature of a polar solvent. The hydration forces are manifested as oscillations that result in a force curve for two approaching surfaces attributed to the "squeezing out" of water molecules. This is not, however, the situation in the clay system studied by Williams et al., where the counterions are as mobile as the water molecules. As a single counterion approaches the clay surface the water molecules, of comparable size of the counterion, may flow around the counterion. It is thus implicit in their interpretation that water molecules must attach themselves more strongly to the surface than the counterions.

In view of the fact that the water molecule is a neutral species with an electric dipole, any electrical interaction with the surface must be stronger for the counterion than for the water. This is readily verified in Tables 1 and 2, where the energy-based weighting factors for the various site states are compared. Those states involving the counterions have site association constants much larger than unity whereas those composed solely of water have constants that are near unity. The inclusion of nearest-neighbor interactions does not alter the preference of the counterions to the water for adsorption. As shown in Table 3, the parameter W_{ij} differs significantly from unity only when counterion−counterion interactions (W_{cc}) are involved. Even though these interactions are repulsive ($W_{cc} < 1$), they are not great enough to overcome the attraction to the site of adsorption in the preference of the counterion over the water molecule.

If one considers the adsorption of the counterion onto the surface as a competition with the water molecules, then one must take into account the much larger concentration of water relative to the counterions. In the present case the ratio is $m_w/m_c \approx 40$. Thus, the distribution of water and counterions in the clay system is a result of two important factors. The first is the larger concentration of the solvent relative to the counterions, and the second is the fact that one is dealing with a highly confined space.

As a quantitative model to support the first factor responsible for the reported distributions, we used a one-dimensional isotherm model that included the nearest-neighbor interactions. The fraction of sites occupied by the specific site states for the fixed concentrations $m_c = 1.42$ and $m_w = 55.5$ were calculated by the finite difference expression (viz. eq 29). We considered four models: five site states with hydrated counterion (model 1); five site states with unhydrated counterion (model 2); three site states with hydrated counterion (model 3); three site states

with unhydrated counterion (model 4). The results are given in Table 4. The total fraction of sites with counterions, whether in layer 1 or layer 2, is less than 15% for all models considered.

Recall that the reason the clays swell is that the counterion becomes hydrated, thereby enticing water into the interplanar region. The electrical interaction of one water molecule with the headgroup is $L_h = 1.3594$ (cf. Table 1). If this is assumed to be the equilibrium constant for the hydration reaction $m_w + m_c = m_{c,h}$, then the relative concentration of the unhydrated to hydrated counterion is $m_c/m_{c,h} = 1/m_w L_h \ll 1$. Therefore the hydrated counterion is the most likely species in solution and site state 4 may be considered as an unlikely state. Elimination of site state 4 also supports the relatively low frequency of appearance of the counterion headgroups in layer 2.

The above arguments may explain the preference of water over the counterion in the first two layers near the clay surface. These results should obtain regardless of the size of the container as long as $m_w \gg m_c$. To explain the maximum in the counterion distribution midway between the clay surfaces one must consider the relative sizes of the adsorbing species and the distance between the clay plates. The relative ratio of the counterion diameter (cylindrical model), water diameter, and plate separation distance is $2r_c:2r_w:2a = 1.07:1:11.3$. If water is preferred in the first two layers, then the "free" volume available for the counterions has a thickness of approximately 22 Å. Considering the possibility that the counterion may have an extension of approximately 18.7 Å (cf. section 3), there is little room for the counterions to exist anywhere else except in the region between the clay plates.

For the purpose of comparison of the choice of the counterion dimensions, we calculated the fraction of sites occupied for the spherical counterion of radius $r_c = 5.3$ Å. Calculations were carried out for model 2 as this model gave the highest counterion coverage for the cylindrical counterion (cf. Table 4). The results for the spherical counterion are summarized in Table 5.

TABLE 5: Fraction of State-Specific Sites Occupied for the Spherical Counterion Model[a]

	θ_1	θ_2	θ_3	θ_4	θ_5	$\theta_2 + \theta_5$	$\theta_3 + \theta_4$
model 2	0.2231	0.3980	0.0302	0.0303	0.3184	0.7164	0.0605

[a] Calculated with the following parameters: $r_c = 5.3$ Å; $r_s = 1.52$ Å; $r_d = 0.75$ Å; $r_w = 1.50$ Å; $Z_s = -1$, $Z_c = +1$; $|\delta Z_w| = 0.26$.

We conclude that the water−counterion distribution between the clay plates as reported by Williams et al.[1] is not inconsistent with the electrostatic principles behind the Poisson−Boltzmann equation. The apparent error is in the PB equation, where the solvent is treated as a dielectric continuum rather than a discrete polar object. The maximum in the distribution of the counterions at the midplate location is attributed to the confinement of the water and counterions to a separation distance comparable to the size of the adsorbing species.

Acknowledgment. I am grateful to Professor Smalley of the Department of Physics and Astronomy at the University College London for discussions regarding his work on clays.

References and Notes

(1) Williams, G. D.; Soper, A. K.; Skipper, N. T.; Smalley, M. V. *J. Phys. Chem. B* **1998**, *102*, 8945.

(2) Enström, S.; Wennerström, H. *J. Phys. Chem.* **1978**, *82*, 2711.

(3) *CRC Handbook of Chemistry and Physics*, 64th ed.; CRC Press: Boca Raton, FL, 1983.

(4) Hill, T. L. *An Introduction to Statistical Thermodynamics*; Dover Publications: New York, 1986.

(5) Schmitz, K. S. *Langmuir* **1999**, *15*, 2854.

(6) Henderson, D.; Lozada-Cassou, M. *J. Colloid Interface Sci*. **1986**, *114*, 180.

(7) Henderson, D. *J. Colloid Interface Sci*. **1988**, *121*, 486.

(8) Henderson, D.; Lozada-Cassou, M. *J. Colloid Interface Sci*. **1994**, *162*, 508.

(9) Trokhymchuk, A.; Henderson, D.; Wasan, D. T. *J. Colloid Interface Sci*. **1999**, *210*, 320.